Supporting Information

Significantly enhanced bioconversion of high titer biomass-derived furfural to furfuryl alcohol by robust endogenous aldehyde reductase in a sustainable way

Junhua Di[a #], Xiaolong Liao[b#], Qi Li[b#], Yu-Cai He*[a,b], Cuiluan Ma[b,*]

[a] *School of Pharmacy & School of Biological and Food Engineering, Changzhou University, Changzhou, P.R. China.*

[b] *State Key Laboratory of Biocatalysis and Enzyme Engineering, Hubei University, Wuhan, P.R. China.*

Corresponding authors emails:

heyucai2001@163.com; yucaihe@cczu.edu.cn **(Y. He);** macuiluan@163.com **(C. Ma)**

Author contribution

They contributed to this work equally.

S1. **Materials and Methods**

S1.1 MD simulation of FAL ligand with FucO

FucO-FAL interactions were analyzed using a commercial molecular docking program (AutoDock Tools 4.2). The MD simulation of FAL ligand with FucO was predicted. Visualization is done by Pymol software.

S1.2 Preparation of solid acid catalyst Sn-CRS

Under the vigorous agitation, dry CRS (20.0 kg) was immersed in a 200-L reactor containing 100 L of 4.0 M H_2SO_4 at 30 ℃ for 3 h. The resulting liquor was regulated to neutrality by addition of NaOH, and H_2SO_4-treated CRS (AT-CRS) was then isolated by filtration and repeatedly washed by using deionized (DI) water to remove the residues of AT-CRS surface. The AT-CRS (6.0 kg, dry weight) were blended with $SnCl_4{\cdot}5H_2O$ (3.0 kg) and ethanol (120.0 L) in a 200-L reactor, and the formed mixture was thoroughly blended via vigorous stirring. Then, the aqueous ammonia (25 wt%) was dripped slowly into this mixture until the pH of this mixture reached 6.0. This liquor was dried in a thermostatic drying oven for 12 h at 70 ℃, and the obtained sample was further dried in this oven (90 ℃) for 12 h. The dried solid was immersed in 50 L of H_2SO_4 (500.0 mM) for 3 h. The acidified solid was then separated from the solution by vacuum filtration. The recovered solid was dried in the thermostatic drying oven (110 ℃) for 3 h and Sn-CRS was obtained by calcination in a muffle furnace at 550 ℃ for 3 h in air.

S1.3 Characterization of solid acid catalysts Sn-CRS

CRS and Sn-CRS solid acid were characterized by means of XRD, FT-IR spectroscopy, SEM, NH_3-TPD, and N_2 adsorption-desorption isotherms analysis.

S1.4 Chemical biological method catalyzes corncob to produce FOL

FAL was synthesized from corn cob using the prepared solid acid catalyst. Corncob (75 g/L) was added into the autoclave reactor (Nanjing Zhengxin Equipment Co., P.R. China) containing 40 mL water, Sn-CRS loading (1.5-3.0 wt%), formic acid (1 wt%)

and reacted at 160-180 ℃ at 5-40 min. Subsequently, the FAL derived from corncob was reduced to FOL by recombinant *Escherichia coli* FF182 under optimal conditions. The formed FAL and FOL was measured using HPLC.

S2. Results and discussion

S2.1 MD simulation of FAL ligand with FucO

Molecular docking (MD) simulation, a potent computational technique, has been currently utilized to predict geometry of protein-ligand complexes. In this work, the MD simulation of FAL ligand with FucO was predicted. The 3D visualization was performed by PyMOL software. Based on the AutoDock 4.2 simulation result (Fig. S2), the FAL displayed -4.4 kcal/mol binding energy at the binding site containing two hydrogen-bonds with interacting amino acid residues Gly14 and Ala178. Overall, binding energy less than 0 kcal/mol suggested that the ligand could bind the receptor spontaneously, whereas the binding energy below -4.25 kcal/mol indicated there was a certain binding activity between the receptor and the ligand. The bond distances between FAL and the respective interacting amino acid residues Gly14 and Ala178 were 2.2 and 2.1 Å, respectively. The above results suggested that ALR in FF182 cells had a high affinity for furfural and good bioreduction activity.

S2.2. Characterization of solid acids Sn-CRS

SEM was utilized to measure the surface structure of CRS (support) and Sn-CRS (catalyst) (Fig. S3). Distinct from the support CRS, catalyst Sn-CRS had voids with rough and fibrous structures, which was ascribed to the sulfonation that could lead to the pore collapse and the enlarged internal pore volume. On the surface of Sn-CRS, the existed particle clumps could be detected, which was attributed to the presence of SnO_2 (Lewis acid site). The pore and surface features of Sn-CRS was determined with BET (Table S7). By compared with CRS, Sn-CRS had an enlarger specific surface area (429.7 m^2/g), bigger pore volume (0.30 cm^3/g), and smaller size of pore (2.89 nm). In the preparation of Sn-CRS, various performance including soaking, sulfonation, and calcination would eliminate organic and inorganic matters on the carrier CRS, which

might expand the pore volume and specific surface area. These alterations would make more Brønsted and Lewis acid sites exposed, promoting the xylose dehydration and further improving the productivity of FAL.

Sn-CRS was subjected to the FT-IR measurement (Fig. S4A). 3,435 cm^{-1} corresponded to the stretching of hydroxyl group (-OH). 2,935 cm^{-1} was associated with symmetric stretching of methyl group ($-CH_3$) and asymmetric stretching of methylene group ($-CH_2$). 1,640 cm^{-1} was associated with the existence of α-chitin in CRS. Two peaks near 836 and 1,475 cm^{-1} were related to the antisymmetric stretching of carbonate (CO_3^{2-}) vibration, suggesting the presence of residual calcium carbonate ($CaCO_3$) in CRS. 1,025 cm^{-1} was associated with the S=O stretching in Sn-CRS, suggesting that the successful loading of sulfonic groups as Brønsted acid sites on heterogeneous catalysts.[4] These sulfonic groups on Sn-CRS might depolymerize xylan in lignocellulose into xylose molecules and further dehydrate xylose to produce FAL. 644 cm^{-1} was related to tin dioxide, which might act as Lewis acid site. After loading Sn ions, the absorption peaks shifted slightly to the low wavenumber direction, which might be caused by the uniform dispersion of tin in CRS. In the XRD spectrum (Fig. S4B), 19.3° and 26.6° (2θ) were assigned to the diffraction peaks of chitin in CRS. The diffraction peak of $CaCO_3$ was located at 2θ= 29.5°. Sn-CRS had diffraction peaks around 2θ=26.5°, 33.9° and 51.8°, which might correspond to tetrahedral tin dioxide. Distinct from CRS, the diffraction peaks of chitin and $CaCO_3$ were not observed in Sn-CRS. After loading, the pore structure was damaged, resulting in the increase of crystallinity in Sn-CRS. The acid strength and acid sites of Sn-CRS were characterized using NH_3-TPD analysis (Fig. S4C). In view of the temperature-programmed desorption (TPD) with ammonia, the weak, medium and strong acid sites on catalysts might be detected at 100−200 °C, 200−400 °C and 400−800 °C, respectively. While Sn-CRS had one main type of acid sites at ～ 165 °C. These acid sites might be associated with the biomass hydrolysis and xylose dehydration reaction, which would have a crucial role in transforming xylan in lignocellulose into xylose and dehydration of xylose into FAL.

Overall, CRS was loose and porous, with a special network of pore structure. Sn-CRS had a fibrous structure with voids. Tin dioxide (Lewis acid sites) and sulfonic acid group (Brønsted acid sites) existed on its rough surface. The chemocatalyst had good thermal stability and was not easy to lose weight in the range of catalytic temperature. After the biobased carrier CRS was loaded with Sn ions and further sulfonated, Sn-CRS obtained larger comparative area and pore volume, which resulted in more catalytic active sites

S2.3. Chemical biological method catalyzes corncob to produce FOL

Furthermore, Sn-CRS loading (1.5-3.0 wt%), performance temperature (160, 170 or 180 °C), and reaction duration (5-40 min) were examined on the effect of FAL formation. The Sn-CRS (2.0 wt%) could give the maximum yield (53.4%) of FAL in water under the temperature of 180 ℃ and microwave of 600 W within 10 min (Fig. S5a & S5b). Industrially, heterogeneous chemocatalysts were often recovered and recycled many times because of their merits of easy recovery and good reusability.[24] In water, Sn-CRS was recovered and recycled. From 1st to 7th run, the yield of FAL was declined from 53.4% to 37.9% (Fig. S5c). The pore structure and active centers of Sn-CRS might be blocked and covered by some organic impurities generated in this catalytic process, which would lower the catalytic activity. While Sn-CRS maintained a high FAL yield after 7 cycles, indicating that Sn-CRS had good reusability. The time-dependence curves for chemoenzymatically catalyzing corncob into FOL under the optimum performance conditions was displayed (Fig. S5d). In 40 mL water, 3.0 g milled corncob (75 g/L), 0.80 g Sn-CRS (2.0 wt%), and 0.40 g formic acid (1.0 wt%) were placed to an autoclave (100-mL, 300 rpm). Under the temperature of 180 ℃ and microwave of 600 W, co-catalysis of corncob (75 g/L) was conducted to yield 103.5 mM FAL (53.4% yield, based on xylan in corncob) within 10 min. The formed FAL solution was fully transformed to FOL within 60 min. Notably, no 2,5-bis(hydroxymethyl)furan was detected after bioreduction.

Figure Captions

Fig. S1. Construction procedure of the recombinant strain containing FucO and FDH (a); Procedures to assemble two genes fucO and fdh with expressing vector [fucO encodes ALR and fdh encodes FDH] (b); SDS-PAGE (c).

Fig. S2. MD snapshots of the binding sites of FucO (a); The magnified docking poses obtained for FAL ligands in the homology model generated for FucO (b); Visualization of FAL with binding pocket of FucO (c).

Fig. S3. SEM image of raw CRS (a) and Sn-CRS (b).

Fig. S4. FTIR image of raw material CRS and Sn-CRS (A); XRD image of raw material CRS and Sn-CRS (B); NH_3-TPD image of Sn-CRS (C).

Fig. S5. Effect of Sn-CRS load on the FAL generation [corncob (75 g/L), Sn-CRS (1.5-3.0 wt%), 0.40 g formic acid (1.0 wt%), 180 °C, 10 min, 600 W] (a); Effects of reaction temperature and duration on the FAL production [corncob (75 g/L), Sn-CRS (2.0 wt%), 0.40 g formic acid (1.0 wt%), 160-180 °C, 5-40 min, 600 W] (b); The test of Sn-CRS reusability [corncob (75 g/L), Sn-CRS (2.0 wt%), 0.40 g formic acid (1.0 wt%), 180 °C, 10 min, 600 W] (c); The time dependence of reaction curves for converting corncob into and FAL and FOL [Chemical conversion: 3.0 g milled corncob (75 g/L), Sn-CRS (2.0 wt%), and 0.40 g formic acid (1.0 wt%), 180 °C, 10 min, 600 W; Biocatalysis: whole-cell 0.1 g/mL, 30 °C, pH 7.0] (d).

Note: $$FAL\ yield(\%) = \frac{FAL\ produced\ (g) \times 0.88 \times 150}{Corncob\ (g) \times 0.341 \times 96} \times 100$$

Fig. S6. Sketch of single ALR expressing vector. **[**FucO was taken as an example for single ALR expressing vector. FucO was inserted in MCS-1 under the control of IPTG-

inducible T7 promoter].

Fig. S7. Structure of plasmid pRSFDuet-FucOrbsFDH.

Fig. S8. SDS-PAGE [Lane 1: Protein of FF182 (as FucO has a predicted molecular weight of 40.5 KDa and FDH has an extremely near predicted molecular weight of 40.3 KDa, thus they can't be separated properly); Lane 2: Protein of AF183 (AdhE has a predicted molecular weight of 96.1 KDa with a weak expression)].

Fig. S9. MS for FOL

Fig. S10. ^{1}H NMR for the prepared FOL.

Table Captions

Table S1. Length of genes or molecular weight of enzymes in this study.

Table S2. Recombinant strains of *E. coli* BL21(DE3) constructed in this study.

Table S3. The stability of reductase in whole-cells under different bioreaction pH and temperature.

Table S4. Primers used in this study.

Table S5. The sequence of FucO and FDH.

Table S6. Related studies about reduction of FAL into FOL via biocatalysis.

Table S7. Surface, pore and catalytic properties of raw material CRS and solid acid Sn-CRS.

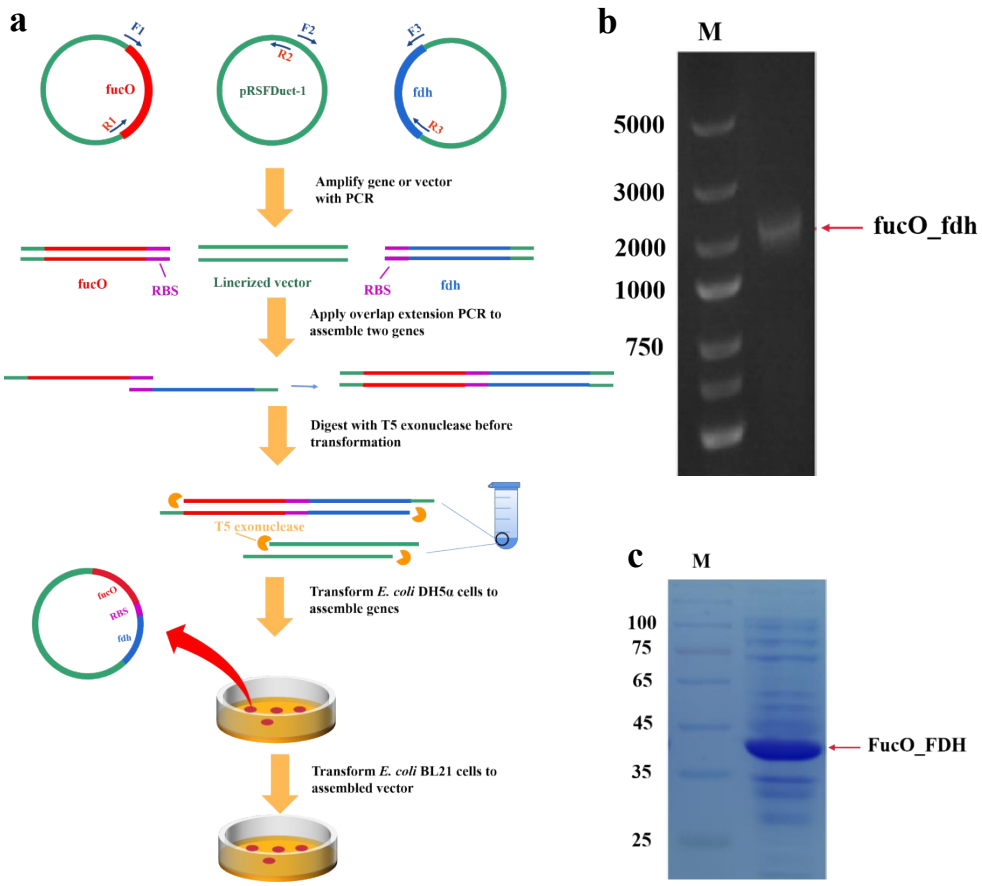

Fig. S1. Construction procedure of the recombinant strain containing FucO and FDH (a); Procedures to assemble two genes fucO and fdh with expressing vector [fucO encodes ALR and fdh encodes FDH] (b); SDS-PAGE (c).

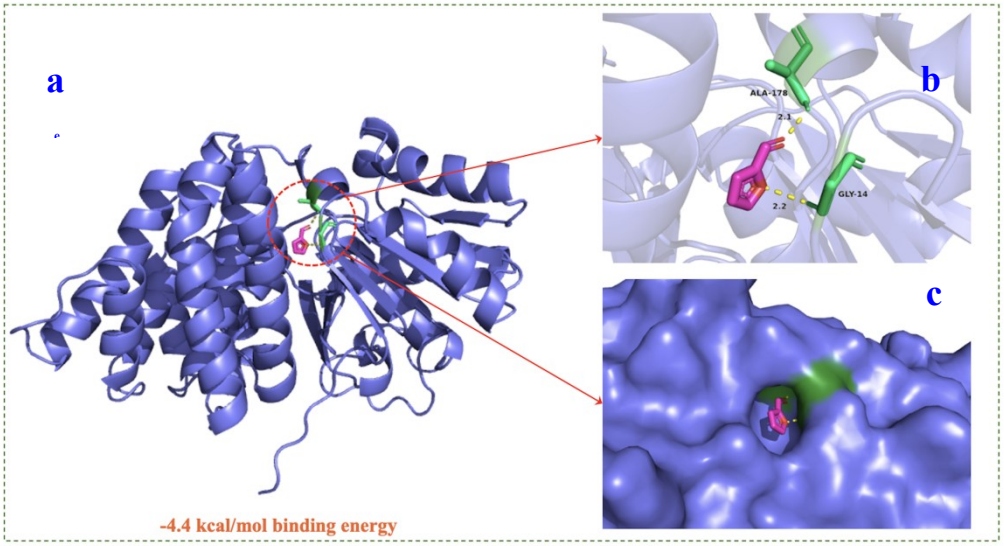

219

220 **Fig. S2.** MD snapshots of the binding sites of FucO (a); The magnified docking poses
221 obtained for FAL ligands in the homology model generated for FucO (b); Visualization
222 of FAL with binding pocket of FucO (c).

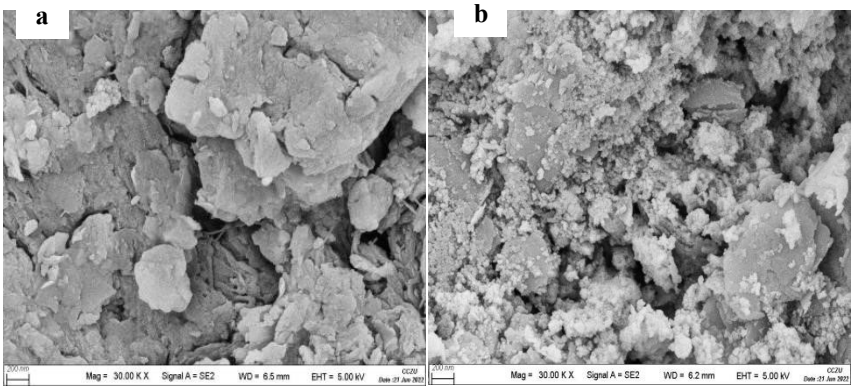

Fig. S3. SEM image of raw CRS (a) and Sn-CRS (b).

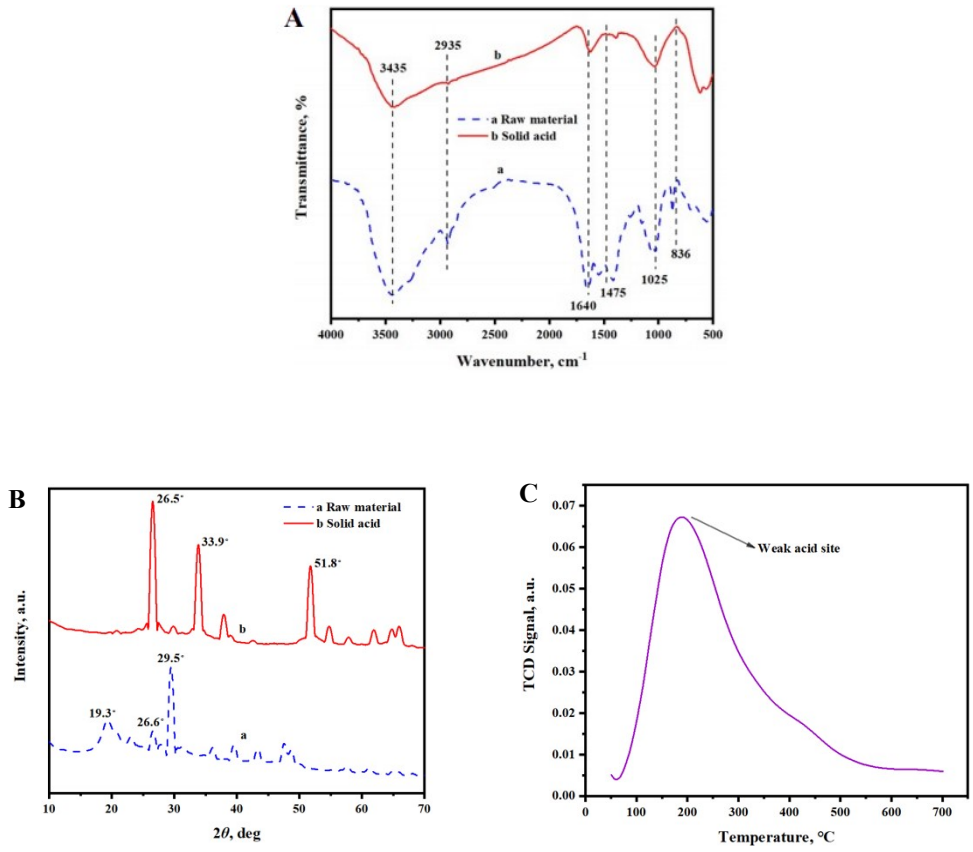

Fig. S4. FTIR image of raw material CRS and Sn-CRS (A); XRD image of raw material CRS and Sn-CRS (B); NH_3-TPD image of Sn-CRS (C).

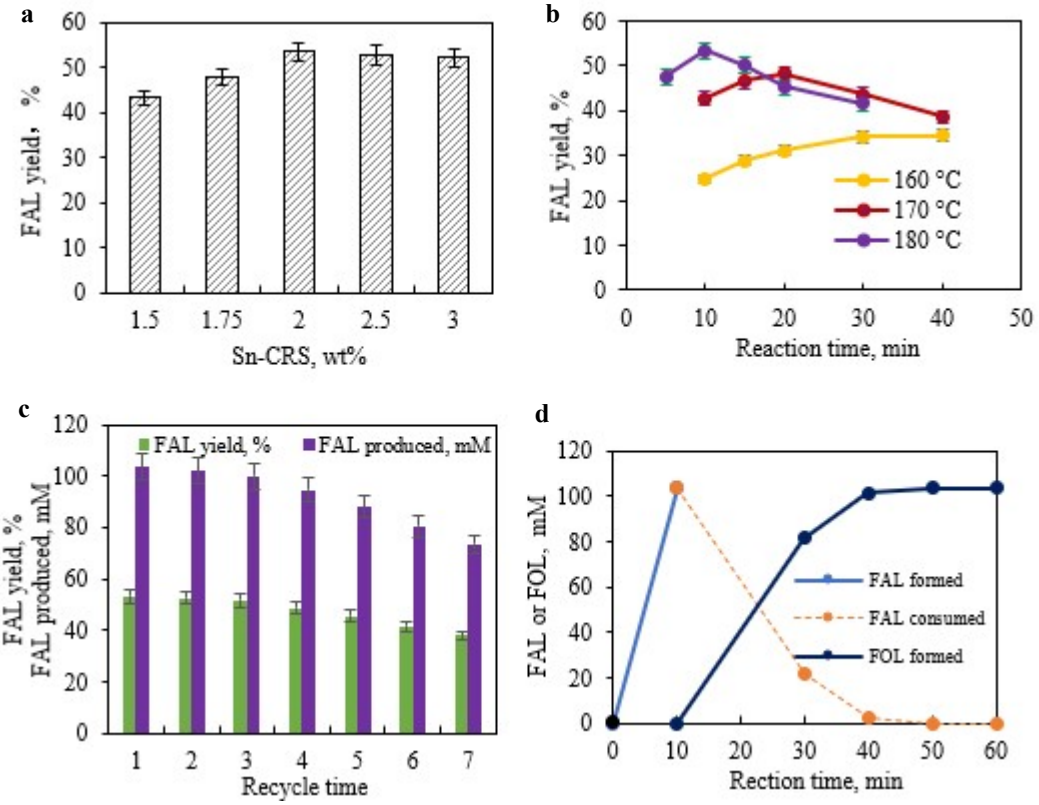

Fig. S5. Effect of Sn-CRS load on the FAL generation [corncob (75 g/L), Sn-CRS (1.5-3.0 wt%), 0.40 g formic acid (1.0 wt%), 180 °C, 10 min, 600 W] (a); Effects of reaction temperature and duration on the FAL production [corncob (75 g/L), Sn-CRS (2.0 wt%), 0.40 g formic acid (1.0 wt%), 160-180 °C, 5-40 min, 600 W] (b); The test of Sn-CRS reusability [corncob (75 g/L), Sn-CRS (2.0 wt%), 0.40 g formic acid (1.0 wt%), 180 °C, 10 min, 600 W] (c); The time dependence of reaction curves for converting corncob into and FAL and FOL [Chemical conversion: 3.0 g milled corncob (75 g/L), Sn-CRS (2.0 wt%), and 0.40 g formic acid (1.0 wt%), 180 °C, 10 min, 600 W; Biocatalysis: whole-cell 0.1 g/mL, 30 °C, pH 7.0] (d).

Note: $$FAL\ yield(\%) = \frac{FAL\ produced\ (g) \times 0.88 \times 150}{Corncob\ (g) \times 0.341 \times 96} \times 100$$

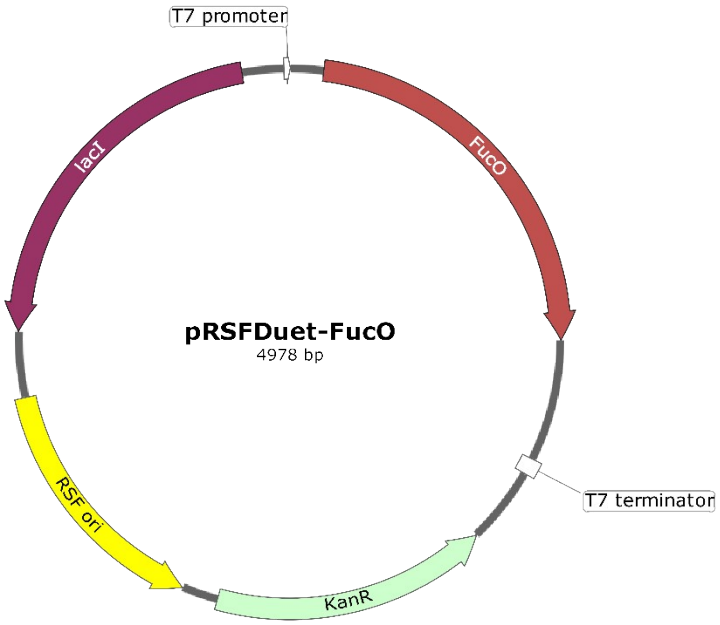

Fig. S6. Sketch of single ALR expressing vector. **[**FucO was taken as an example for single ALR expressing vector. FucO was inserted in MCS-1 under the control of IPTG-inducible T7 promoter].

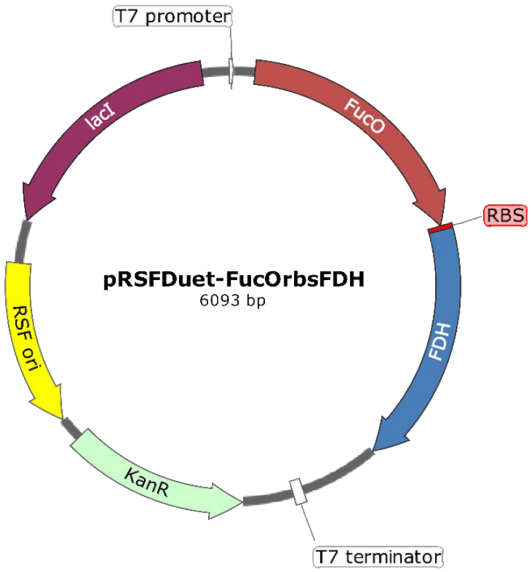

Fig. S7. Structure of plasmid pRSFDuet-FucOrbsFDH.

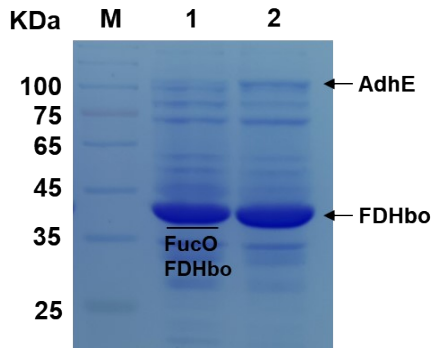

Fig. S8. SDS-PAGE [Lane 1: Protein of FF182 (as FucO has a predicted molecular weight of 40.5 KDa and FDH has an extremely near predicted molecular weight of 40.3 KDa, thus they can't be separated properly); Lane 2: Protein of AF183 (AdhE has a predicted molecular weight of 96.1 KDa with a weak expression)].

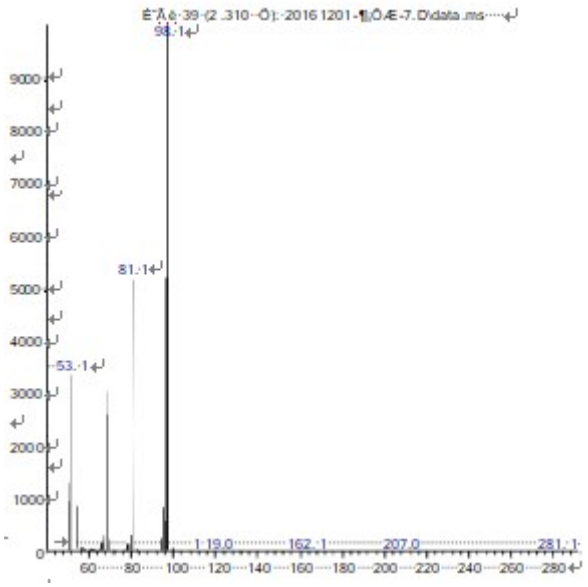

Fig. S9. MS for FOL

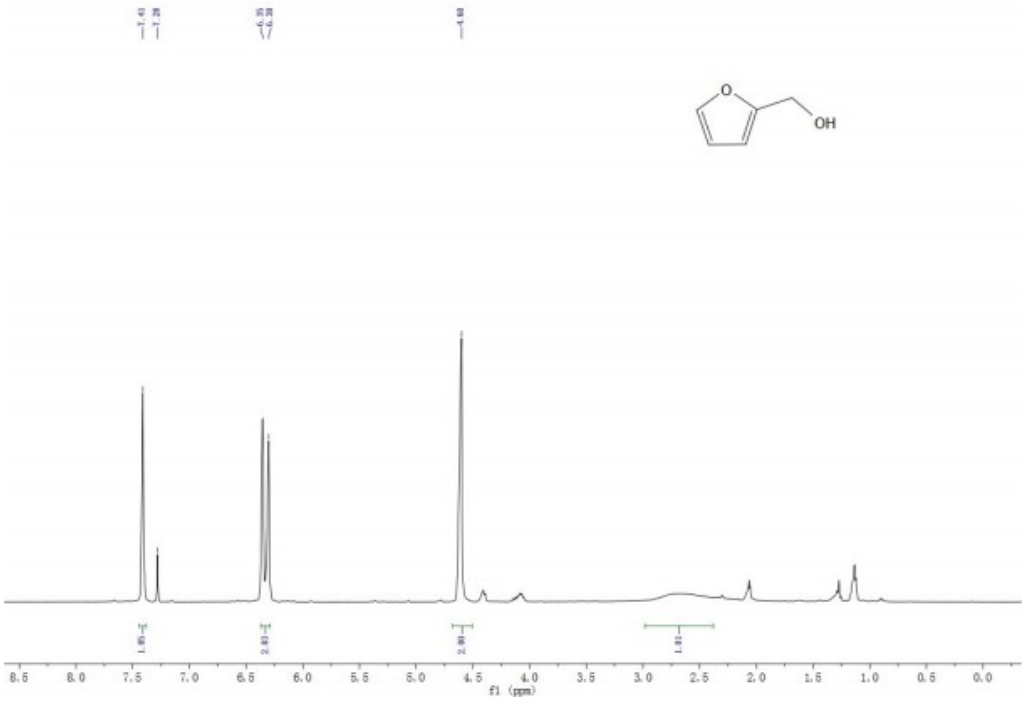

Fig. S10. ^{1}H NMR for the prepared FOL.

Table S1. Length of genes or molecular weight of enzymes in this study.

Name	Length (bp)	Molecular weight (Kda)
YiaY	1152	40.4
YjgB	1020	36.5
AdhE	2676	96.1
YqhD	1164	42.1
AdhP	1011	35.5
EutE	1404	49.0
DkgA	828	31.1
BetA	1671	61.8
YahK	1050	38.0
GldA	1104	38.7
FucO	1149	40.5
EutG	1188	41.0
YbbO	810	29.4
YghA	885	31.5
FDH	1095	40.3

410

411

412 **Table S2.** Recombinant strains of *E. coli* BL21(DE3) constructed in this study.

Name	Plasmid
AdhE	pRSFDuet-AdhE
AdhP	pRSFDuet-AdhP
BetA	pRSFDuet-BetA
DkgA	pRSFduet-DkgA
EutE	pRSFDuet-EutE
EutG	pRSFDuet-EutG
FucO	pRSFDuet-FucO
GldA	pRSFDuet-GldA
YahK	pRSFDuet-YahK
YbbO	pRSFDuet-YbbO
YghA	pRSFDuet-YghA
YiaY	pRSFDuet-YiaY
YjgB	pRSFDuet-YjgB
YqhD	pRSFDuet-YqhD
FF182	pRSFDuet-FucOrbsFDH

413

414

Table S3. The stability of reductase in whole-cells under different bioreaction pH and temperature.

pH	Temperature	$t_{1/2}$
6.5	30 °C	1.9 day
7.0		2.5 day
7.5		1.6 day
7.0	4 °C	3.8 day
	30 °C	2.5 day
	45 °C	0.42 day

419

420 **Table S4.** Primers used in this study.

Name of primers	Sequence
AdhE-F	caccatcatcaccacATGGCTGTTACTAATGTCGCTGAACTT
AdhE-R	attcggatcctggctTTAAGCGGATTTTTTCGCTTTTTTCTCAGC
AdhP-F	caccatcatcaccacATGAAGGCTGCAGTTGTTACGAAGG
AdhP-R	attcggatcctggctTTAGTGACGGAAATCAATCACCATGCG
BetA-F	caccatcatcaccacTTGCAATTTGACTACATCATTATTGGTGCC
BetA-R	attcggatcctggctTCATTTTTTCGCTCTCACCGGCATC
DkgA-F	caccatcatcaccacATGGCTAATCCAACCGTTATTAAGCTACAGG
DkgA-R	attcggatcctggctTTAGCCGCCGAACTGGTCAGG
EutE-F	caccatcatcaccacATGAATCAACAGGATATTGAACAGGTGGTG
EutE-R	attcggatcctggctTTAAACAATGCGAAACGCATCGACTAATAC
EutG-F	caccatcatcaccacATGCAAAATGAATTGCAGACCGCG
EutG-R	attcggatcctggctTTATTGCGCCGCTGCGTACAG
FucO-F	caccatcatcaccacATGGCTAACAGAATGATTCTGAACGAAACG
FucO-R	attcggatcctggctTTACCAGGCGGTATGGTAAAGCTCT
GldA-F	caccatcatcaccacATGGACCGCATTATTCAATCACCGG
GldA-R	attcggatcctggctTTATTCCCACTCTTGCAGGAAACGC
YahK-F	caccatcatcaccacATGAAGATCAAAGCTGTTGGTGCATATTCC
YahK-R	attcggatcctggctTCAGTCTGTTAGTGTGCGATTATCGATAAC
YbbO-F	caccatcatcaccacATGACTCATAAAGCAACGGAGATCCTGAC
YbbO-R	attcggatcctggctTCACCCCTGCAATATTTTGTCCATCAC
YghA-F	caccatcatcaccacATGTCTCATTTAAAAGACCCGACCACG
YghA-R	attcggatcctggctTTAACCTAAATGCTCGCCGCCG
YiaY-F	caccatcatcaccacATGGCATCTTCAACTTTCTTTATTCCTTCTGTG
YiaY-R	attcggatcctggctTTACATCGCTGCGCGATAAATCG
YjgB-F	caccatcatcaccacATGTCGATGATAAAAAGCTATGCCGCAA
YjgB-R	attcggatcctggctTCAATAATCGGCTTTCAACACCACGC

YqhD-F	caccatcatcaccacATGAACAACTTTAATCTGCACACCCCAAC
YqhD-R	attcggatcctggctTTAGCGGGCGGCTTCGTATATACG
FucOrbs-R	gatatatctccttaggtaccTTACCAGGCGGTATGGTAAAGCTCT
RbsFDHbo-F	ggtacctaaggagatatatcATGAAAATTGTTCTGGTTCTGTATGATGCAGG
RbsFDH-F	ggtacctaaggagatatatcATGAAAATTGTTCTGGTTCTGTATGATGCAGG
FDH-R	attcggatcctggctTCATTTTTTGTCGTGTTTGCCATAGGC
pRSFDuet-F	AGCCAGGATCCGAATTCGAGC
pRSFDuet-R	GTGGTGATGATGGTGATGGCTGC
CpRSFDuet-F	GCAGCCATCACCATCATCACCAC
CpRSFDuet-R	GCTCGAATTCGGATCCTGGCT

The underlined sequences in lowercase are used for assembly meditated by T5 exonuclease, the sequences highlighted in green contains ribosome site and are also used for overlap PCR) DNA sequences of codon-optimized enzyme.

425 **Table S5.** The sequence of FucO and FDH.

Sequence
FucO
atggctaacagaatgattctgaacgaaacggcatggtttggtcggggtgctgttggggctttaaccgatgaggtgaaac
gccgtggttatcagaaggcgctgatcgtcaccgataaaacgctggtgcaatgcggcgtggtggcgaaagtgaccgata
agatggatgctgcagggctggcatgggcgatttacgacggcgtagtgcccaacccaacaattactgtcgtcaaagaag
ggctcggtgtattccagaatagcggcgcggattacctgatcgctattggtggtggttctccacaggatacttgtaaagcga
ttggcattatcagcaacaacccggagtttgccgatgtgcgtagcctggaagggctttccccgaccaataaacccagtgta
ccgattctggcaatccccaccacagcaggcactgcggcagaagtgaccattaactacgtgatcactgacgaagaaaaa
cggcgcaagtttgtttgcgttgatccgcatgatatcccgcaggtggcgtttattgacgctgacatgatggatggtatgcctc
cagcgctgaaagctgcgacgggtgtcgatgcgctcactcatgctattgaggggtatattacccgtggcgcgtgggcgct
aaccgatgcactgcacattaaagcgattgaaatcattgctggggcgctgcgaggatcggttgctggtgataaggatgcc
ggagaagaaatagcgctcgggcagtatgttgcgggtatgggcttctcgaatgttgggttagggttggtgcatggtatggc
gcatccactgggcgcgttttataacactccacacggtgttgcaaacgccatcctgctaccgcatgtcatgcgctataacg
ctgactttaccggtgagaagtaccgcgatatcgcgcgcgttatgggcgtgaaagtggaaggtatgagcctggaagagg
cgcgtaatgccgctgttgaagcggtgtttgctctcaaccgtgatgtcggtattccgccacatttgcgtgatgttggggtacg
caaggaagacattccggcactggcgcaggcggcactgaatgatgtttgtaccggtggcaacccgcgtgaagcaacgc
ttgaggatattgtagagctttaccataccgcctggtaa
FDH
atgaaaattgttctggttctgtatgatgcaggtaaacatgcagcagatgaagaaaaactgtatggctgcaccgaaaataaa
ctgggtattgcaaattggctgaaagatcagggtcatgaactgattaccaccagtgataaagaaggtggtaatagcgttct
ggatcagcatattccggatgccgatattatcattaccacaccgtttcatccggcatatatcaccaaagaacgtatcgacaa
agccaaaaaaactgaaactggttgttgttgccggtgttggtagcgatcatattgatctggattatatcaatcagaccggcaaa
aaaatcagcgtgctggaagttaccggtagcaatgttgttagcgttgcagaacatgttgttatgaccatgctggttctggtgc
gcaattttgttccggcacatgagcagattattaaccatgattgggaagttgcagccattgcaaaagatgcctatgatattga
aggtaaaaccattgcaaccattggtgcaggtcgtattggttatcgtgttctggaacgtctggttccgtttaatccgaaagaa
ctgctgtattatgattatcaggcactgccgaaagatgccgaagaaaaagttggtgcccgtcgtgttgaaaatattgaagaa
ctggttgcacaggccgatattgttaccgttaatgcaccgctgcatgccggtacaaaaggtctgattaacaaagagctgct
gagcaaattcaaaaaaggtgcatggctggttaataccgcacgtggtgcaatttgtgttgccgaagatgttgcagcagcac

tggaaagcggtcagctgcgtggttatggtggtgatgtttggtttccgcagccagcaccgaaagatcatccgtggcgtgat
atgcgtaacaaatatggtgccggtaatgcaatgacaccgcattatagcggtacaaccctggatgcacagacccgttatg
cacagggcaccaaaaacattctggaaagttttttttaccggcaaattcgattatcgtccgcaggatattattctgctgaatggt
gaatatgtgaccaaagcctatggcaaacacgacaaaaaatga

426

427

Table S6. Related studies about reduction of FAL into FOL via biocatalysis.

Catalyst	Substrate	Substrate concentration	Time	Product yield	Reference
M. guilliermondii	FAL	200 mM	7 h	80%	45
S. cerevisiae	FAL	50 mM	24 h	88%	46
B. coagulans	FAL	40 mM	24 h	95%	47
CCZU-A13 cells	FAL	200 mM	12 h	94%	48
CCZU-K14 cell	FAL	200 mM	24 h	100%	49
FF182 cell	FAL	300 mM	3 h	100%	-

Table S7 Surface, pore and catalytic properties of raw material CRS and solid acid Sn-CRS.

Solid sample	BET surface area (m^2/g)	Pore volume (cm^3/g)	Pore size (nm)
Raw material CRS	94.1	0.11	4.65
Sn-CRS	429.7	0.30	2.89